Chemical Lasers and Kinetics

David F. Hakala
NanoTekniks
October 2026

Abstract

In 1976, in my third year of graduate school, I was given the opportunity, and honor, of teaching a January term short course in Chemical Lasers. About 7 or 8 students signed up to take it. I put together a draft of course material covering basic laser operation and theory and then focused on the operation and kinetics of how a chemical laser worked with some specific examples. I worked in the group of Paul Harteck and Robert Reeves and one of the earlier developments in that lab was the iodine lamp operating at a wavelength of 206.2 nm. We also had one of the experimental racks set up with the capability to generate a nitrogen afterglow. I ran some experiments in which I introduced iodine vapor to the flowing nitrogen afterglow and observed emission at 206.2 nm. This raised in my mind the possibility of creating an electronic chemical laser. This paper reformats the original draft material of the Chemical Laser short course and examines the issues associated with creating a chemical laser based on the N+NI reaction.

Chemical lasers draw both their excitation energy and their population inversion from exothermic chemical reactions. This paper outlines the conditions for optical gain and uses a simple rate-equation model to show how the competition among pumping, radiative transitions, and vibrational energy transfer decides whether, and for how long, a chemical system can lase. It reviews the HF lasers produced by flash photolysis of N_2F_4 + RH mixtures as an example of extracting kinetic information from laser emission. It then considers the N + NI reaction as a possible pump for an electronic-transition iodine chemical laser at 206.2 nm and identifies the long-lived I($^2P_{1/2}$) lower level as the main obstacle. Three lasers developed after 1974, the F + H_2 (HF) laser, the chemical oxygen–iodine laser (COIL), and the all-gas-phase iodine laser (AGIL), are then described with their reaction mechanisms, rate equations, gain conditions, and layouts, and a numerical model shows the time course of a pulsed HF laser.

The 206.2 nm iodine line itself is then reviewed: the Harteck–Reeves–Thompson iodine lamp, the enhancement of the line by rare-gas metastables, and the Xe–I_2 and He–I_2 discharge lamps of Lomaev and Tarasenko. These lead to a proposed nitrogen-afterglow experiment to measure whether N + NI can pump the 206.2 nm upper level selectively, with a kinetic model of the flow tube that sets where the reaction should be observed and shows how the measured emission profile yields the rate constant of N + I_2 and the branching fraction of N + NI.

A final analysis of the lower-level removal rate shows that an inversion on the 206.2 nm line is very unlikely with collisional removal and afterglow pumping rates. The experiment is therefore best viewed as a measurement of the energy disposal of N + NI rather than as a laser test. A postscript summarizes some later chemical laser developments.

Introduction

A chemical laser is a laser in which the excitation energy and the population inversion are supplied by a chemical reaction. As early as 1961, J. C. Polanyi suggested that laser action might occur in $HCl^{\dagger}$ that is vibrationally and rotationally inverted as a result of the reaction between H atoms and Cl_2.[1] Kasper and Pimentel observed the first chemical laser action, in $HCl^{\dagger}$ formed by the flash photolysis of H_2–Cl_2 mixtures.[2]

Photodissociation lasers, in which the excited species that lase are formed directly in the primary photolysis, are not considered chemical lasers but form a class by themselves. In many cases flash photolysis or a pulsed electrical discharge is used to create radicals or excited species, which then react to produce the excited species in which laser action occurs. This latter type is considered a "pure" chemical laser.

Electronically and/or vibrationally excited states are known to be formed as products of many highly exothermic reactions. Some examples of reactions leading to electronically excited states are

$$NO + O + M \rightarrow NO_2^* + M; \qquad NO_2^* \rightarrow NO_2 + h\nu_F$$
$$SO + O + M \rightarrow SO_2^* + M; \qquad SO_2^* \rightarrow SO_2 + h\nu_F$$
$$N + NI \rightarrow N_2^* + I$$

To date, however, no chemical laser operating on an electronic transition has been developed. Most emit in the infrared, on vibrational transitions. Because of their relatively high exothermicity, the hydrogen halide reactions were among the first investigated. Table 1 lists some reactions that lead to laser action, together with their reaction enthalpies. Unfortunately, the efficiency of converting vibrational quanta into emitted photons is low because of relaxation and the competing processes of vibration–vibration (V→V) and vibration–translation (V→T) energy transfer, which are often fast enough to deplete the excited state and prevent laser action altogether.

Table 1. Reactions leading to chemical laser action. SI values added.

Reaction	ΔH_{rxn} (kcal/mol)	ΔH_{rxn} (kJ/mol)
$H + Cl_2 \rightarrow HCl^{\dagger} + Cl$	−47	−197
$Cl + HI \rightarrow HCl^{\dagger} + I$	−34	−142
$H + Br_2 \rightarrow HBr^{\dagger} + Br$	−43	−180
$H + F_2 \rightarrow HF^{\dagger} + F$	−98[a]	−410[a]
$Cl + HBr \rightarrow HCl^{\dagger} + Br$	−16	−67
$H + ClNO \rightarrow HCl^{\dagger} + NO$	−65	−272
$O + CS \rightarrow CO^{\dagger} + S$ [b]	−87	−363
$H + ClN_3 \rightarrow HCl^{\dagger} + N_3$	−66	−276
$CH + O \rightarrow CO^{\dagger} + H$	−176	−736
$CH + NO \rightarrow CO^{\dagger} + NH$	−105	−439

[a] Corrected from −90 kcal/mol in the typescript, using $D_0(HF) \approx 135$ and $D_0(F_2) \approx 37$ kcal/mol.
[b] Replaces the typescript's SO + CS → CO + S_2 (−53 kcal/mol). O + CS is the established CO-laser pumping reaction; its 0 K reaction enthalpy is about −3.76 eV, and the CO is formed with an inverted vibrational distribution peaking near v = 12–13.[16]

Details of Laser Action

The central role kinetics plays in deciding whether a chemical system will lase becomes clearer when the physical situation is examined in more detail.

As light passes through a medium with an extinction coefficient per unit length k, the absorption is described by a Beer's-law equation:

$$\frac{I}{I_0} = e^{-kx}$$

or, in differential form,

$$-\frac{1}{I}\frac{dI}{dx} = k.$$

Under ordinary photochemical conditions $k = \sigma n$, where σ is the absorption cross section (cm^2 per particle) and n is the number density (particles per cm^3). However, when the excited state may be appreciably populated, the correct form is

$$k = \bar{\sigma}\left(n_1 - \frac{g_1}{g_2}\, n_2\right)$$

where $\bar{\sigma}$ is the absorption cross section averaged over the band in question, n_2 and n_1 are the populations of the upper and lower states, and g_2 and g_1 are the corresponding degeneracies. Also,

$$\bar{\sigma} = \frac{h\nu}{c\,\Delta\nu}\, B$$

where ν is the transition frequency, $\Delta\nu$ the bandwidth, and B the Einstein coefficient for stimulated absorption or emission.[3] If

$$\frac{n_2}{g_2} > \frac{n_1}{g_1}$$

then k is negative and one has negative absorption, or gain: the intensity of light increases as it passes through the medium because of stimulated emission from the population-inverted state.

Consider laser transitions between two vibrational levels. The degeneracy of a vibrational level is one, and that of a rotational level is $(2J + 1)$. Even when the total vibrational populations satisfy $n_1 > n_2$, laser action can occur on individual P-branch transitions, since $(2J_2 + 1) < (2J_1 + 1)$. The underlying reason is that each vibrational level holds its own rotational (Boltzmann) distribution. A P-branch line P(J) connects the upper level (v, J−1) to the lower level (v−1, J), and for equal rotational constants B the lower level lies higher in rotational energy by $2BJ$. With equal rotational temperatures in the two levels, the line has gain whenever

$$\frac{N_v}{N_{v-1}} > \exp\left(-\frac{2BJ\,hc}{kT}\right)$$

which can be satisfied at sufficiently high J even when $N_v < N_{v-1}$ (Fig. 1). This effect, known as partial inversion, was predicted by Polanyi[1,9] and is observed in almost all chemical laser transitions, because rapid vibrational relaxation makes absolute population inversions hard to achieve.

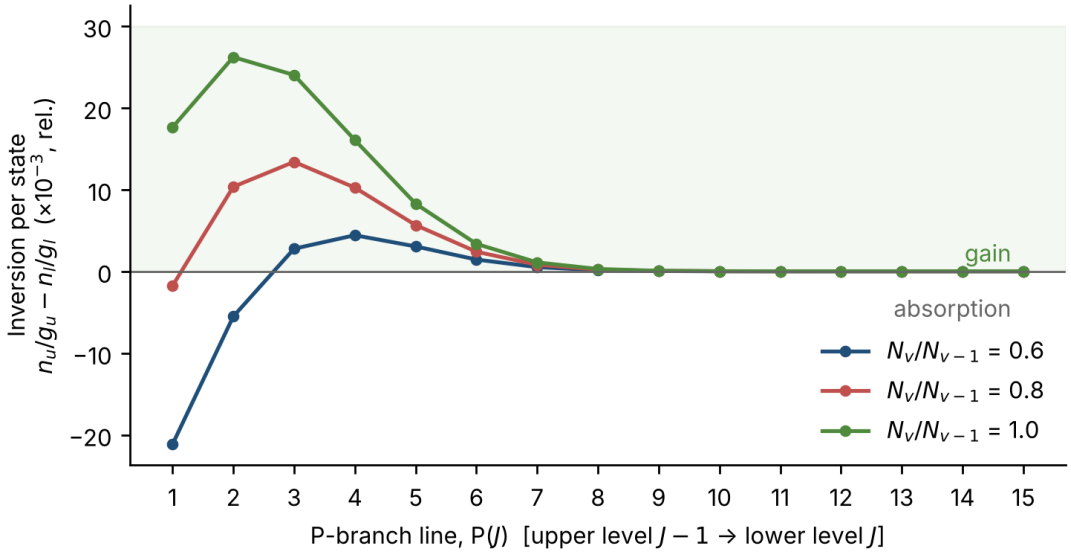


Figure 1. Partial inversion on HF P-branch lines ($B \approx 20.9$ cm^{-1}, $T = 300$ K) for three ratios of total vibrational population. Lines above zero have gain even when the vibrational levels are not inverted. (Added in the 2026 revision.)

When the gain exceeds the optical losses of the system, self-sustained laser action can occur. Obtaining the population inversion and maintaining it are direct results of the kinetics of the system. The upper-state population n_2 is set by its rate of formation by reaction and its loss rates through emission, relaxation, and energy transfer. Most chemical lasers operate in a pulsed mode because n_1 builds up with time and laser action stops. The exception is the continuous-wave HF laser demonstrated at The Aerospace Corporation in 1969,[10] in which supersonic mixing and rapid flow carry de-excited molecules out of the optical cavity before the lower level can fill. By varying the pressure and other parameters and observing how the laser intensity (and therefore the system's gain) responds, one can in principle extract the rate constants of the system.

As a simplified example, consider the reaction scheme

$$\mathrm{A + BC \rightarrow AB}(v{=}2) + \mathrm{C} \qquad (k_1)$$

$$\mathrm{AB}(v{=}2) \rightarrow \mathrm{AB}(v{=}1) + h\nu_\mathrm{F} \qquad (k_2)$$

$$\mathrm{AB}(v{=}2) + \mathrm{AB}(v{=}0) \rightarrow 2\ \mathrm{AB}(v{=}1) \qquad (k_3)$$

$$\mathrm{AB}(v{=}2) + \mathrm{M} \rightarrow \mathrm{AB}(v{=}1) + \mathrm{M} \qquad (k_4)$$

The first step is the pumping reaction that produces the excited species. The second is the radiative transition that can lead to laser action under suitable conditions. Steps three and four are competing processes that deplete AB(v=2) by vibration→vibration and vibration→translation energy transfer, respectively. The rate equations for this system are

$$\frac{d[\mathrm{AB}(v=2)]}{dt} = k_1[\mathrm{A}][\mathrm{BC}] - k_2[\mathrm{AB}(v=2)] - k_3[\mathrm{AB}(v=2)][\mathrm{AB}(v=0)] - k_4[\mathrm{AB}(v=2)][\mathrm{M}]$$

$$I = \frac{d(h\nu_F)}{dt} = k_2[\mathrm{AB}(v=2)]$$

$$\frac{d[\mathrm{AB}(v=1)]}{dt} = 2k_3[\mathrm{AB}(v=0)][\mathrm{AB}(v=2)] + k_2[\mathrm{AB}(v=2)] + k_4[\mathrm{AB}(v=2)][\mathrm{M}]$$

$$\frac{d[\mathrm{AB}(v=0)]}{dt} = -k_3[\mathrm{AB}(v=2)][\mathrm{AB}(v=0)]$$

The last equation completes the set. These equations describe the medium below laser threshold. Once oscillation begins, stimulated emission becomes the dominant loss of AB(v=2), at a rate proportional to the cavity photon density and to $(n_2 - n_1)$, and it must be added to the equations for v=2 and v=1.

If the initial concentrations of A and BC and the effective concentration of the quenching body M are known, these equations can be solved for [AB(v=2)] as a function of time. Qualitatively, the v=0 and v=1 populations are small at first, and the v=2 population builds up until it is large enough to produce observable laser action. As the lower vibrational levels fill, however, two things happen: depletion of v=2 speeds up, and the ratio of v=2 to v=1 falls. The population inversion is destroyed, and this is the main reason laser action stops.

Figure 2 shows what these equations predict for a specific system, the F + H_2 → HF laser (AB = HF), using measured rate data rather than illustrative values. The model includes levels v = 0–3, the measured F + H_2 product distribution, HF self-relaxation, V→V exchange, and, unlike the equations above, stimulated emission into a laser cavity. It is described more fully in the section on the HF laser below. The total inversion between v = 2 and v = 1 forms within a fraction of a microsecond, and lasing begins at about 0.15 μs. The stimulated emission then cascades the population down the vibrational ladder, and the pulse is over in about 4 μs.

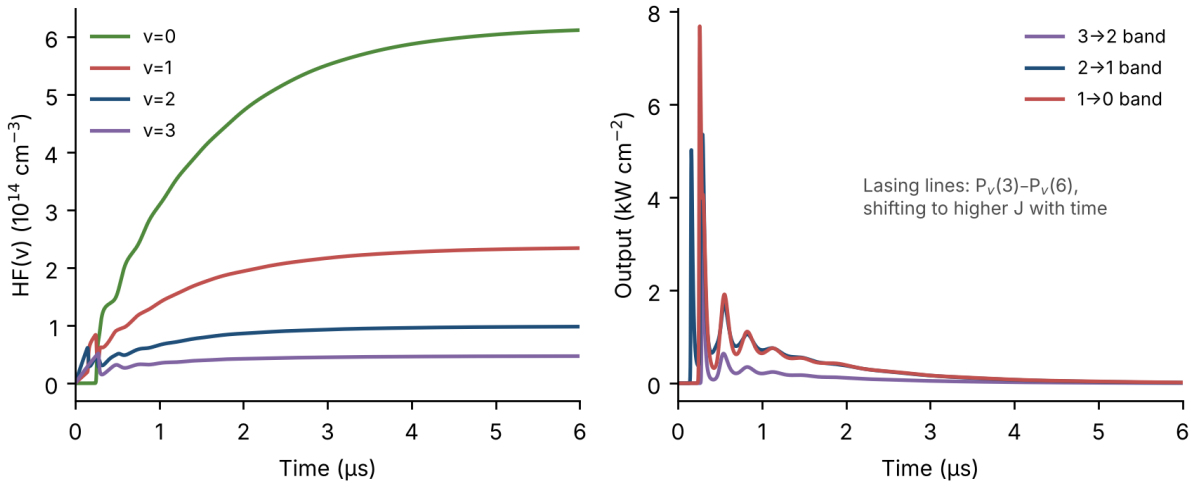


Figure 2. Pulsed F + H_2 → HF laser modeled with measured rate data. Left: HF(v) populations. Right: output on the 3→2, 2→1, and 1→0 bands. Conditions: 300 K; 0.13 kPa (1 torr) H_2 with He diluent; 1 × 10^{15} cm^{-3} F atoms formed instantly at t = 0; F + H_2 rate constant 2.5 × 10^{-11} cm^3 s^{-1} with $f_1 : f_2 : f_3$ = 0.31 : 1 : 0.47; HF–HF V→T 1.7 × 10^{-12} v cm^3 s^{-1} (ref. 15); HF–HF V→V 1 × 10^{-11} cm^3 s^{-1} (order-of-magnitude estimate); 50 cm gain length; 80% output coupler. Lasing is taken on the highest-gain P-branch line of each band, with the rotational populations in equilibrium.

Real systems are much more complicated. For example, the v=1 level is also depleted by collisions, and the pumping reaction generally populates all the energetically accessible vibrational levels of

the product molecule, so the assumption that the v=1 population is initially zero is not valid. In the H_2–Cl_2 system the vibrationally excited HCl comes from the H + Cl_2 step of the chain. Anlauf et al.[4] measured the relative rates of formation of HCl into each vibrational level for this reaction by infrared chemiluminescence. They found a distribution peaking at v = 3, with formation into v = 1 only about one-fifth as fast as into v = 3, and about 45% of the available energy appearing as vibration. On that distribution, about 25% of the HCl product is formed in v = 2 and 10% in v = 1, and correspondingly more is formed in v = 3 and above. One therefore expects the population inversion to be very hard to maintain for any length of time. (At 1–25 torr (0.13–3.3 kPa) with flashlamp excitation, pulse durations are of the order of 10–100 μs.)

As this simplified example shows, time-resolved measurements of the pulse intensity, together with measurements of the total pulse emission as a function of reactant concentrations, can give specific and valuable information on the rate constants k_1 through k_4. Knowing one or more of them simplifies the problem, but in real systems this information is often hard to extract quantitatively.

Specific Chemical Systems

It is useful at this point to discuss some specific chemical systems, their experimental conditions, and the interpretation of the results.

HF lasers from N_2F_4 + RH photolysis

The first system is the chemical laser produced by flash photolysis of N_2F_4 + RH mixtures, examined by M. C. Lin of the Naval Research Laboratory.[5] The experimental arrangement is shown in Fig. 3.

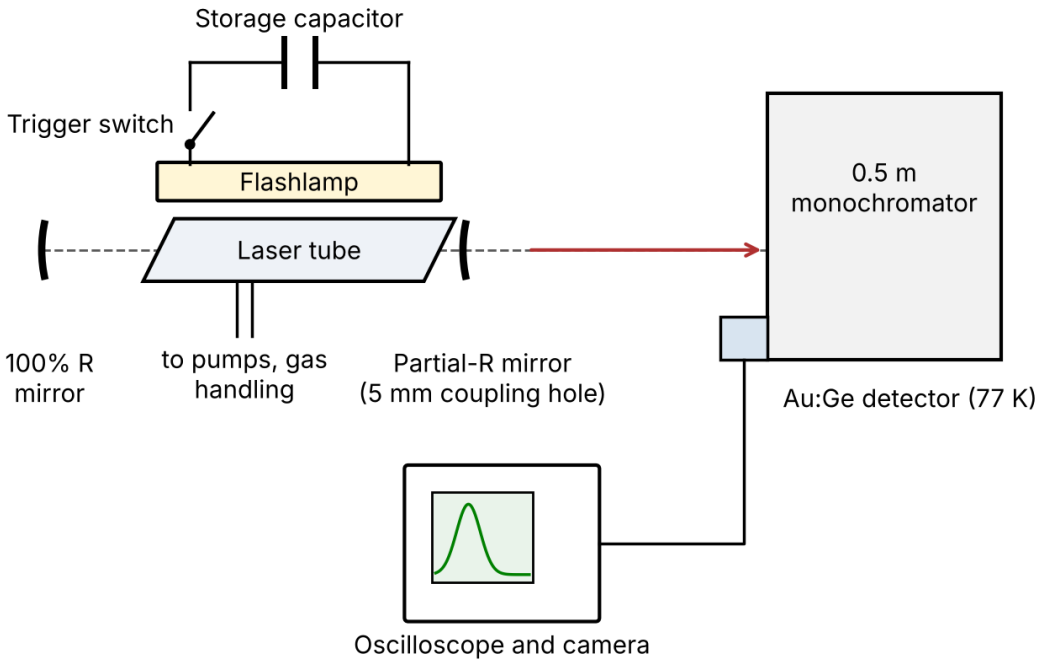


Figure 3. Experimental arrangement of Lin (redrawn from the original hand sketch).

Laser emission was found on several vibrational–rotational lines of HF. At room temperature N_2F_4 is in equilibrium with the free radical NF_2. NF_2 absorbs at 2500–2700 Å (250–270 nm) and is the light-absorbing species. It can dissociate by two pathways:

$$NF_2(^2B_1) \rightarrow F(^2P) + NF(^1\Delta)$$
$$NF_2(^2B_1) \rightarrow F(^2P) + NF(^3\Sigma)$$

To account for the products found by mass spectrometric analysis, the following mechanism was proposed for photolysis of pure N_2F_4:

Reaction	Rate parameter
$N_2F_4 \rightleftharpoons 2\ NF_2$	K_{eq}
$N_2F_4 + h\nu \rightarrow N_2F_3 + F$	$\lambda < 2100$ Å (210 nm), I_1
$NF_2 + h\nu \rightarrow NF(^3\Sigma \text{ or } ^1\Delta) + F$	$\lambda = 2500–2700$ Å (250–270 nm), I_2
$2\ NF \rightarrow N_2 + 2\ F$	k_1
$F + N_2F_4 \rightarrow NF_3 + NF_2$	k_2
$NF + N_2F_4 \rightarrow NF_2 + N_2F_2 + F$	k_3
$2\ F + M \rightarrow F_2 + M$	k_4

In the presence of RH, however, hydrogen abstraction by F dominates and the last four reactions are effectively suppressed. The proposed mechanism is then:

Reaction	Rate constant
$F + RH \rightarrow HF^\dagger + R$	k_5
$R + N_2F_4 \rightarrow RNF_2^\dagger + NF_2$	k_6
$RNF_2^\dagger \rightarrow 2\ HF^\dagger + R'CN$	k_{6a}
$RNF_2^\dagger + M \rightarrow RNF_2 + M$	k_{6b}
$R + N_2F_4 \rightarrow RF + N_2F_2 + F$	k_7
$NF + RH \rightarrow RNFH^\dagger$	k_8
$RNFH^\dagger \rightarrow HF^\dagger + R''–CH{=}NH$	k_{8a}
$RNFH^\dagger + M \rightarrow RNFH + M$	k_{8b}

Reaction 5 has been studied by many authors and is known to be a fast and efficient source of $HF^\dagger$. Reaction 6 has also been studied; it is fast, and once enough activation energy is supplied it is very efficient at eliminating $HF^\dagger$ through 6a (about 90% eliminate $HF^\dagger$). The other steps are supported by Lin's mass spectrometric analysis, which showed the products they form.

$HF^\dagger$ can be produced by three of these reactions: 5, 6, and 8. Reaction 5 is believed to be the principal pumping reaction. For RH = H_2 it gives the population ratios $N_2/N_1 = 3.2$ and $N_1/N_0 \rightarrow 1$, an absolute population inversion with high potential gain, whereas reaction 6 as studied gives $N_1/N_0 = 0.35$, with low maximum gain.[6]

Among the RH species used, HCl and CH_3F relaxed $HF^\dagger$ rapidly, which sets a lower limit on those relaxation rate constants. For RH = C_2H_5I, the flash also dissociated the iodide, $C_2H_5I \rightarrow C_2H_5 + I^*$,

where I* denotes I($5^2P_{1/2}$). The absence of any 1.3 μm emission from I* implies that collisional quenching, or a chemical reaction such as

$$I^* + N_2F_4 \rightarrow NF_2I + NF_2$$

is faster than the time needed to reach laser threshold, again setting a lower limit on the rate constants.

Running a series of closely related compounds, rather than the fairly different ones Lin used, might have produced data more readily interpreted in terms of a trend. As this shows, getting readily interpretable data from such a system is difficult, and the experiment must be designed carefully to get the most out of it.

Designing a chemical laser: N + NI

As a digression, consider applying kinetics to the design of a chemical laser. As mentioned above, the reaction

$$N + NI \rightarrow N_2^* + I$$

can produce an electronically excited N_2 molecule, in the metastable $A^3\Sigma_u^+$ state. Phillips studied the reaction of active nitrogen with I_2 and deduced a mechanism for the formation of N_2*, with energy transfer to I_2 and subsequent bright blue fluorescence.[7,8] The reaction is about 189–191 kcal/mol (791–799 kJ/mol) exothermic, which raises the possibility of forming excited iodine in the I($5p^4(^3P_2)6s\ ^2[2]_{3/2}$) level, 56 093 cm^{-1} above the ground state, followed by emission of the non-resonance 2062 Å (206.2 nm) line to I($5p^5\ ^2P^\circ_{1/2}$). (The typescript labeled this level "6 $^2P_{3/2}$"; it belongs to the $5p^46s$ configuration, built on the $^3P_2$ state of the I^+ core.) The relevant levels are shown in Fig. 4. The 2062 Å line was not observed to any great extent in earlier experiments, but in work done during the January term I measured it as the strongest emission, by an order of magnitude, from a reaction tube in which N atoms and I_2 are mixed. This raises the possibility of an electronic chemical laser in a region very close to the vacuum ultraviolet.

A reaction scheme such as

$$(1) \qquad N + I_2 \rightarrow NI + I$$

$$(2) \qquad N + NI \rightarrow N_2 + I(6s\ ^2[2]_{3/2})$$

$$(3) \qquad I(6s\ ^2[2]_{3/2}) \rightarrow I(^2P_{1/2}) + h\nu_1$$

$$(4) \qquad I(^2P_{1/2}) \rightarrow I(^2P_{3/2}) + h\nu_2$$

might be proposed. Assuming constant concentrations of N atoms (from the condensed discharge) and of I_2, one can solve this system for I($6s\ ^2[2]_{3/2}$) and I($^2P_{1/2}$) as functions of time. (One can also include quenching steps 3a and 4a, in which the two excited states are quenched by a body M of constant concentration.) Writing N_u and g_u for the population and degeneracy of I($6s\ ^2[2]_{3/2}$), and N_l and g_l for those of I($5p^5\ ^2P^\circ_{1/2}$), the earlier discussion shows that if at any time t

$$N_u / g_u \qquad > \qquad N_l / g_l$$

laser action could occur, since the system has gain. With

$$g_u = 2J + 1 = 4\ (J = 3/2), \qquad g_l = 2J + 1 = 2\ (J = 1/2)$$

the required population inversion is

$$N_u > 2\,N_l.$$

Under the actual conditions no laser action is observed. The difficulty is the lower level. I($^2P_{1/2}$) is metastable, with a radiative lifetime of about 0.1 s, so without a fast removal process it accumulates and the 206.2 nm transition is self-terminating. If, however, one could find a "resonance" quenching reaction that more or less selectively depopulates the $^2P_{1/2}$ level of I, a continuous laser might be possible. As shown later, however, the removal would have to be extremely fast, because the upper level radiates in nanoseconds (see "The lower-level removal requirement and the prospects for inversion").

Ground-state O_2 is a natural candidate. Its $a^1\Delta_g$ state lies only about 279 cm^{-1} above I($^2P_{1/2}$) (Fig. 4), so the near-resonant exchange

$$I(^2P_{1/2}) + O_2(X^3\Sigma_g^-) \rightleftharpoons I(^2P_{3/2}) + O_2(a^1\Delta_g)$$

is fast and would empty the lower laser level directly. Run in reverse, with chemically generated $O_2(a^1\Delta_g)$, this same exchange became the pump of the chemical oxygen–iodine laser in 1978[11] (see Postscript). A practical scheme would also have to keep O_2 from quenching I(6s $^2[2]_{3/2}$) and N_2(A), so the quenching rate constants for those species would be the first measurements to make.

Pulsed operation is no easier. Because the upper level radiates in nanoseconds, the lower level catches up within a few nanoseconds of the start of pumping, far faster than a chemical pump can act. This is analyzed quantitatively below.

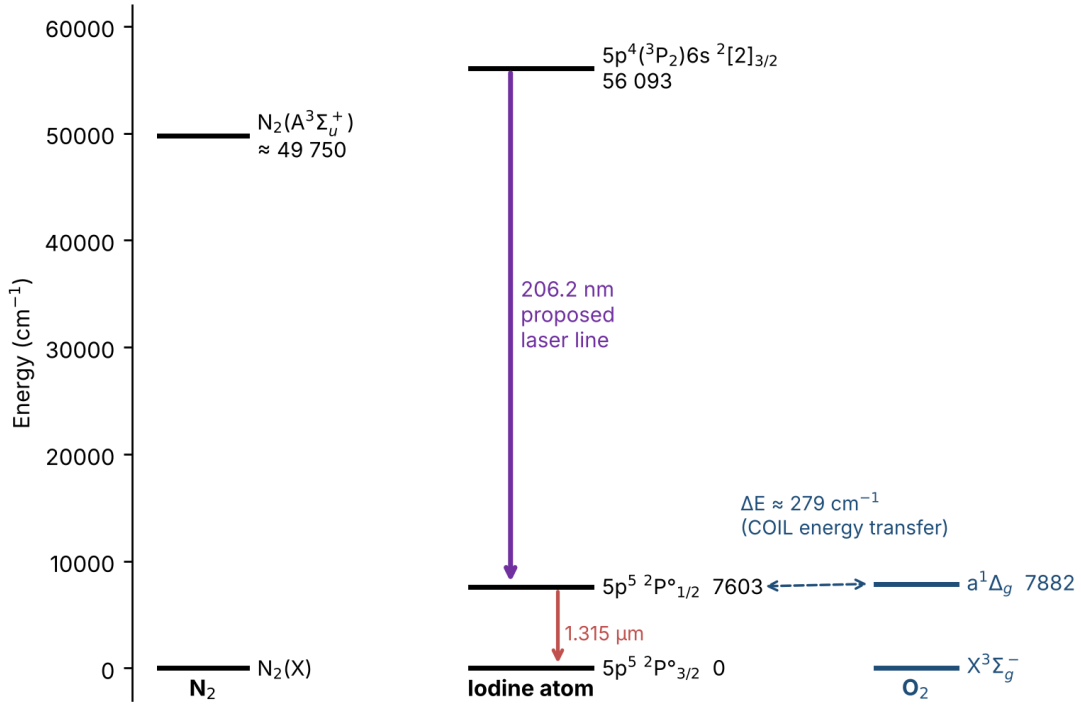


Figure 4. Energy levels relevant to the proposed N + NI iodine laser: the 206.2 nm transition from I(6s $^2[2]_{3/2}$) to I($^2P_{1/2}$), the 1.315 μm I($^2P_{1/2}$) → I($^2P_{3/2}$) transition, $N_2(A^3\Sigma_u^+)$, and the near-resonant $O_2(a^1\Delta_g)$ level. (Added in the 2026 revision.)

Practical Chemical Lasers: HF, COIL, and AGIL

The chemical lasers that were developed furthest after 1974 illustrate the ideas of this paper on a large scale. The HF laser, pumped by F + H_2, lases on vibrational transitions. The chemical oxygen–iodine laser (COIL) lases on an electronic transition of atomic iodine and is the practical realization of the $O_2(a^1\Delta_g)$–iodine coupling discussed above. The all-gas-phase iodine laser (AGIL) pumps the same iodine transition with a nitrogen–halogen energy carrier, $NCl(a^1\Delta)$, and is the closest relative of the N + NI scheme.

The HF (F + H_2) laser

Chemistry. In the continuous-wave (CW) form of the laser, fluorine atoms are produced thermally in a combustor. Deuterium is burned in excess F_2 (or NF_3) diluted with helium, which gives a hot, partly dissociated, F-rich gas:

$$D_2 + F_2 \rightarrow 2\ DF \qquad \Delta H \approx -130\ \text{kcal/mol}$$

$$F_2 + M \rightleftharpoons 2\ F + M$$

(Deuterium is used in the combustor so that the DF formed there does not absorb on the HF laser lines.) The F atoms are expanded through an array of supersonic nozzles, which cools the gas and "freezes" the atom concentration. H_2 is injected at the nozzle exits, and the pumping reactions take place as the two streams mix:

$$F + H_2 \rightarrow HF(v \le 3) + H \qquad \Delta H \approx -32\ \text{kcal/mol}\ (-133\ \text{kJ/mol}) \qquad \text{(cold reaction)}$$

$$H + F_2 \rightarrow HF(v \le 6) + F \qquad \Delta H \approx -98\ \text{kcal/mol}\ (-410\ \text{kJ/mol}) \qquad \text{(hot reaction, when } F_2 \text{ is present)}$$

The cold reaction has a rate constant of about 2.5×10^{-11} cm^3 s^{-1} at 300 K and forms HF in v = 1, 2, and 3 in the ratio of about 0.31 : 1 : 0.47, with almost nothing in v = 0. It therefore produces a strong *total* inversion between v = 2 and v = 1. The hot reaction, $k \approx 3.5 \times 10^{-12}$ cm^3 s^{-1} at 300 K, puts most of its product in v = 5 and 6.[15] When F_2 is present the two reactions form a chain, and pulsed H_2–F_2 lasers can convert far more chemical energy to light than the initiating pulse supplies.

Losses. The principal deactivation processes are

$$HF(v) + M \rightarrow HF(v-1) + M \qquad (V \rightarrow T)$$

$$HF(v) + HF(0) \rightarrow HF(v-1) + HF(1) \qquad (V \rightarrow V)$$

$$HF(v) + F \rightarrow HF(v-1) + F \qquad (V \rightarrow T,\ \text{partly reactive})$$

Self-relaxation of HF is fast: $k(1 \rightarrow 0) \approx 1.7 \times 10^{-12}$ cm^3 s^{-1} at 300 K, and it increases with v (in proportion to v in the harmonic-oscillator approximation).[15] This is why the lasing zone is kept at low pressure (a few kPa) and why HF should not be allowed to accumulate in the optical cavity.

Rate equations. For the vibrational populations N_v (v = 0–3) in the lasing zone, with f_v the fraction of F + H_2 products formed in level v,

$$\frac{dN_v}{dt} = f_v\, k_F[\mathrm{F}][\mathrm{H_2}] - \left(A_v + \sum_M k_{v,M}^{VT}\,[\mathrm{M}]\right)N_v + \left(A_{v+1} + \sum_M k_{v+1,M}^{VT}\,[\mathrm{M}]\right)N_{v+1} + R_v^{VV} - c\,\gamma_v \Phi_v + c\,\gamma_{v+1}\Phi_{v+1}$$

where A_v is the Einstein coefficient of the v → v−1 band, R_v^{VV} collects the V→V exchange terms, Φ_v is the cavity photon density on the v → v−1 band, and γ_v is the gain of the line that is lasing on that band. The photon density obeys

$$\frac{d\Phi_v}{dt} = c(\gamma_v - \gamma_{th})\Phi_v + \beta A_v N_v, \qquad \gamma_{th} = \frac{1}{2L}\ln\frac{1}{R_1 R_2} + \alpha_{loss}$$

where L is the gain length, R_1 and R_2 are the mirror reflectivities, α_{loss} covers scattering and other losses, and β is the small fraction of spontaneous emission that enters the cavity mode.

Gain on a P-branch line. If the rotational levels are in equilibrium at temperature T, the population of level (v, J) is

$$N_{v,J} = N_v \frac{(2J+1)\,hcB_v}{kT} \exp\left[-\frac{hcB_v J(J+1)}{kT}\right]$$

and the small-signal gain at line center of $P_v(J)$, the line from (v, J−1) to (v−1, J), is

$$\gamma_v(J) = \frac{\lambda^2 A_{v,J}}{8\pi}\, g(\nu_0)\left[N_{v,J-1} - \frac{2J-1}{2J+1}\, N_{v-1,J}\right]$$

where $g(\nu_0)$ is the line-shape function at line center, which is Doppler-dominated at low pressure. This is the general form of the partial-inversion condition of Fig. 1. Because the bracket favors high J, a laser running on a fixed band tends to move to higher J as the lower level fills ("J-shifting").

What the HF laser looks like in practice. Figure 2 solves these equations for a pulsed F + H_2 laser, using the Cohen–Bott rate data. Lasing begins about 0.15 μs after initiation, first on the 2→1 band, then on 3→2 and 1→0, and lasts about 4 μs. The output shows relaxation oscillations and then cascades down the vibrational ladder as each band's lower level fills, with the active lines moving from P(3) to P(6). The calculation also shows why the 1974 flashlamp pulses lasted 10–100 μs: there the pulse length is set by the duration of the flash, which keeps producing F atoms, not by the much faster kinetics of the HF itself. The CW layout is shown in Fig. 5. Because the resonator axis is perpendicular to the flow, the flow carries the de-excited HF out of the optical cavity within microseconds to tens of microseconds, before it can accumulate. That is how the CW laser escapes the bottleneck that terminates pulsed operation.

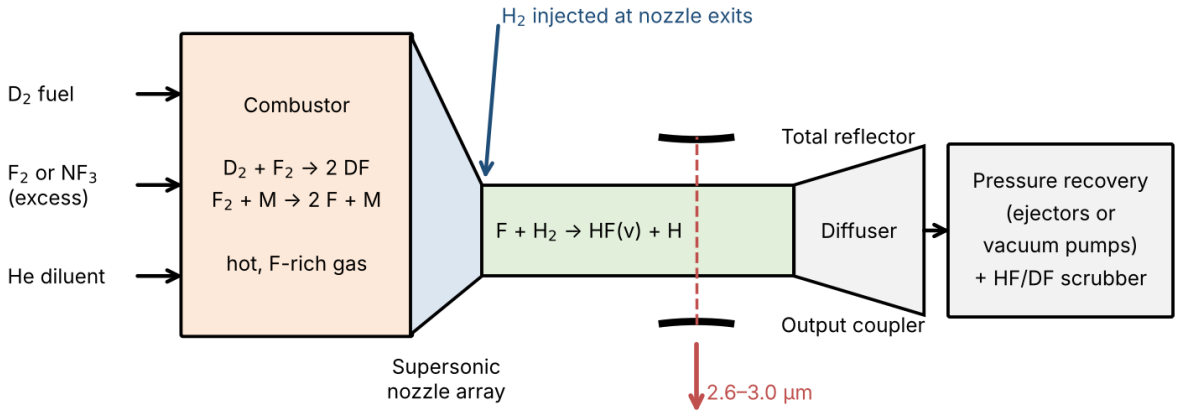


Figure 5. Layout of a continuous-wave supersonic-mixing HF chemical laser. The optical axis runs across the flow; the D_2 combustor supplies hot F atoms, H_2 is injected at the nozzle exits, and HF(v) is formed and lases in the mixing zone before the gas is slowed in the diffuser and pumped away.

The chemical oxygen–iodine laser (COIL)

Singlet-oxygen generation. COIL stores its energy in $O_2(a^1\Delta_g)$, 7882 cm^{-1} (0.98 eV) above the ground state. Its radiative lifetime is of the order of an hour, so it can be made in a liquid-phase reactor and carried a long way in a flowing gas. Chlorine gas reacts with basic hydrogen peroxide (BHP; H_2O_2 + KOH):

$$H_2O_2 + OH^- \rightleftharpoons HO_2^- + H_2O$$

$$Cl_2 + 2\ HO_2^- \rightarrow O_2(a^1\Delta_g) + H_2O_2 + 2\ Cl^-$$

$$\text{net:} \quad Cl_2 + H_2O_2 + 2\ KOH \rightarrow O_2(a^1\Delta_g) + 2\ KCl + 2\ H_2O$$

In the liquid, the $O_2(a^1\Delta_g)$ yield is close to 100%.[17] The generator is run cold so that little water vapor, a strong quencher, is carried downstream.

Iodine dissociation. Molecular iodine is injected near the nozzle throat and is dissociated by the singlet oxygen itself, in a chain that uses several $O_2(a^1\Delta_g)$ molecules for each I_2:[17]

$$I_2 + O_2(a^1\Delta_g) \rightarrow I_2(v) + O_2(X)$$

$$I_2(v) + O_2(a^1\Delta_g) \rightarrow 2\ I + O_2(X)$$

$$I(^2P_{1/2}) + I_2 \rightarrow I(^2P_{3/2}) + I_2(v) \qquad \text{(chain carrier)}$$

$$2\ O_2(a^1\Delta_g) \rightarrow O_2(b^1\Sigma_g^+) + O_2(X); \qquad O_2(b) + I_2 \rightarrow 2\ I + O_2(X)$$

Pumping and lasing. The excitation of iodine is the near-resonant exchange already proposed above as a quencher, run in the pumping direction:

$$I(^2P_{3/2}) + O_2(a^1\Delta_g) \rightleftharpoons I(^2P_{1/2}) + O_2(X^3\Sigma_g^-) \qquad k_f \approx 7.8 \times 10^{-11}\ cm^3\ s^{-1}$$

$$I(^2P_{1/2},\ F' = 3) + h\nu \rightarrow I(^2P_{3/2},\ F'' = 4) + 2\ h\nu \qquad (\lambda = 1.315\ \mu m)$$

The forward exchange is so fast that the iodine populations come to equilibrium with the oxygen in the gain region, with[17]

$$K_{eq} = \frac{k_f}{k_r} = 0.75 \exp\left(\frac{402\ \text{K}}{T}\right) \quad \Rightarrow \quad \frac{[I_{1/2}]}{[I_{3/2}]} = K_{eq}\ \frac{[O_2(a)]}{[O_2(X)]}$$

where $[I_{1/2}]$ and $[I_{3/2}]$ denote the concentrations of $I(^2P_{1/2})$ and $I(^2P_{3/2})$.

The degeneracies of the two iodine levels are 2 and 4, so the gain is

$$\gamma = \sigma\left([I_{1/2}] - 1/2\ [I_{3/2}]\right)$$

where σ is the stimulated-emission cross section of the $F' = 3 \rightarrow F'' = 4$ hyperfine component. Gain therefore requires $[I_{1/2}]/[I_{3/2}] > ½$. In terms of the singlet-oxygen yield $Y = [O_2(a)]/([O_2(a)] + [O_2(X)])$, this becomes

$$Y > Y_{th} = \frac{1}{1 + 2K_{eq}}$$

which is about 15% at 295 K and lower at the low temperatures of a supersonic flow. This is why COIL uses a supersonic nozzle: cooling the gas raises K_{eq}, lowers the threshold yield, and lets more of the stored $O_2(a^1\Delta_g)$ energy be extracted.

Losses. The main losses are quenching of $I(^2P_{1/2})$ by water ($k \approx 2 \times 10^{-12}$ cm^3 s^{-1}), energy pooling of $O_2(a^1\Delta_g)$ ($k \approx 2.5 \times 10^{-17}$ cm^3 s^{-1}), and quenching of $O_2(a^1\Delta_g)$ by water and I_2.[17] The layout in Fig. 6 reflects them: a cold generator, a water trap, late iodine injection, and a short transit to the resonator.

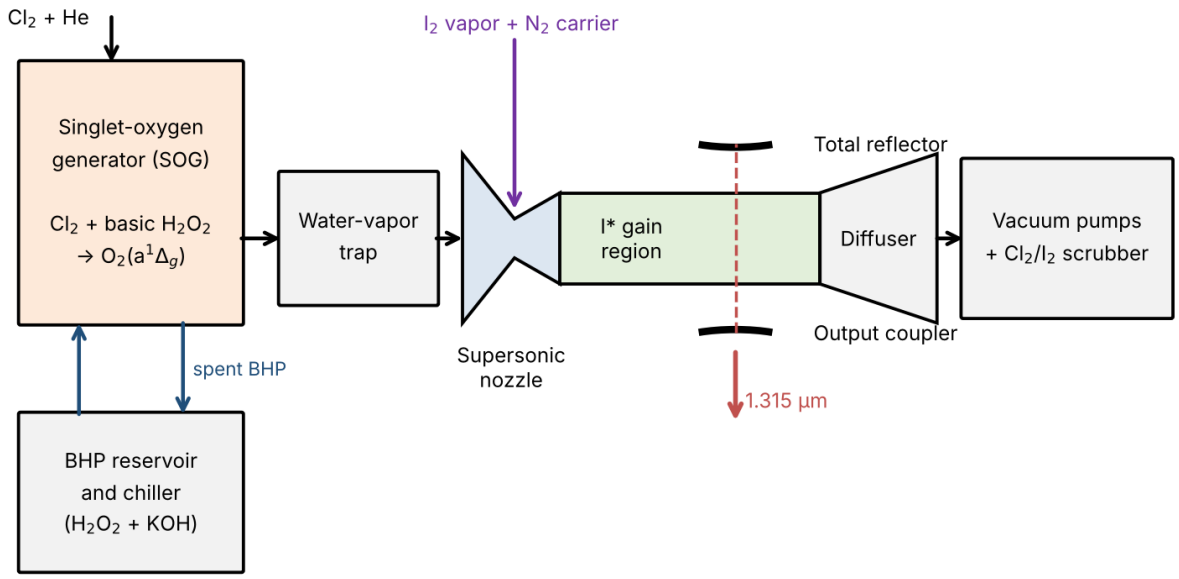


Figure 6. Layout of a supersonic chemical oxygen–iodine laser (COIL). Singlet oxygen made from Cl_2 and basic hydrogen peroxide passes through a water-vapor trap, is mixed with I_2 at the nozzle, and pumps atomic iodine in the gain region; the resonator axis is perpendicular to the flow.

Connection to the N + NI proposal. COIL is a working example of the strategy this paper suggested for iodine, namely choosing a chemical energy store that is nearly resonant with an atomic iodine level. It works on the 1.315 µm transition because $O_2(a^1\Delta_g)$ can both pump the upper level and, through the reverse reaction, keep the population ratio set by the equilibrium constant. The 206.2 nm scheme proposed above would need the same kind of help, but at the other end of the transition: a fast, selective way to empty the lower level.

The all-gas-phase iodine laser (AGIL)

Origin. COIL's singlet-oxygen generator is a gas–liquid reactor using chlorine and concentrated basic hydrogen peroxide. That chemistry is heavy, corrosive, and hard to handle in aircraft or space. The all-gas-phase iodine laser (AGIL) was developed at the U.S. Air Force Research Laboratory to replace it with an all-gas energy carrier. The first continuous-wave device, patented by Henshaw, Hager, Berman, and Madden (filed July 2000, issued October 2002), lased at up to 180 mW.[14] A larger subsonic device later reached 15 W,[23] and a supersonic version was patented in 2008.[24]

Energy carrier. The carrier is NCl in its metastable $a^1\Delta$ state, the isovalent analog of $O_2(a^1\Delta_g)$. $NCl(a^1\Delta)$ lies about 1 700 cm^{-1} above $I(^2P_{1/2})$, so the energy transfer to iodine is exothermic and effectively one-way. This differs from the near-resonant $O_2(a)$–I exchange, so there is no equilibrium threshold of the COIL type: every NCl(a) that transfers its energy produces an $I(^2P_{1/2})$ atom.

Chemistry. In the first device everything was made in a single flow reactor:[14]

$$NF_3 + He \rightarrow F + \text{products } (\approx 10 \text{ kW DC discharge})$$

$$F + DCl \rightarrow DF + Cl \text{ (chlorine-atom source)}$$

$$Cl + HI \rightarrow HCl + I(^2P_{3/2}) \text{ (iodine-atom source; DI may replace HI)}$$

$$Cl + HN_3 \rightarrow HCl + N_3$$

$$Cl + N_3 \rightarrow NCl(a^1\Delta) + N_2(X^1\Sigma_g^+)$$

$$NCl(a^1\Delta) + I(^2P_{3/2}) \rightarrow NCl(X^3\Sigma^-) + I(^2P_{1/2})$$

$$I(^2P_{1/2}) + h\nu \rightarrow I(^2P_{3/2}) + 2\ h\nu\ (1.315\ \mu m)$$

The patent also lists alternative routes, for example $D + NCl_3 \rightarrow NCl_2 + DCl$ followed by $D + NCl_2 \rightarrow DCl + NCl(a^1\Delta)$, and transfer through O_2, $NCl(a^1\Delta) + O_2 \rightarrow O_2(a^1\Delta_g) + NCl(X)$, followed by the usual COIL pumping step.[14]

Apparatus and conditions. The first AGIL (Fig. 7) was a transverse subsonic flow reactor with the resonator axis across the flow.[14]

- **F atoms:** made by the DC discharge in NF_3/He.
- **Injection sequence:** DCl, HI, and then HN_3 (stored as a 10% mixture in He) were injected in that order downstream of the discharge.
- **Flows:** NF_3 2.4 mmol/s, DCl 2.0 mmol/s, HI 0.07 mmol/s, and HN_3 2.0–5.3 mmol/s, at a total pressure of 16 torr (2.1 kPa).
- **Pressure control:** an N_2 flow injected 1.5 m downstream of the cavity through a 3 cm choke orifice.
- **Gain measurement:** 7 cm downstream of the HN_3 injector.
- **Resonator:** two mirrors of 5 m radius with R = 0.99998, plus output couplers between 0.99998 and 0.9979.

The 20 cm subsonic reactor of the later work measured a peak small-signal gain of 2.5×10^{-4} cm^{-1} and extracted 15 W.[23]

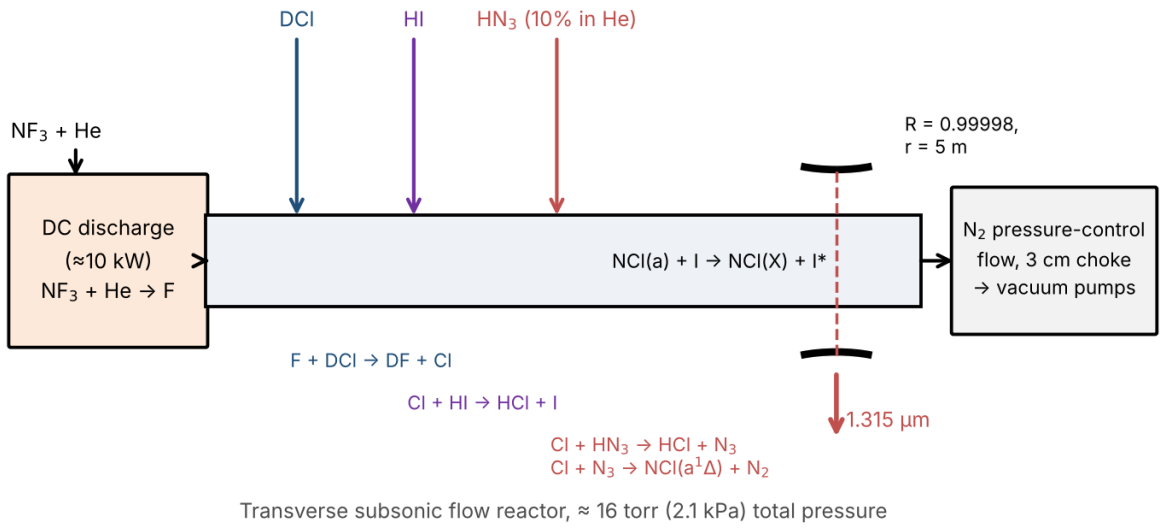


Figure 7. Layout of the first continuous-wave all-gas-phase iodine laser (AGIL), after U.S. Patent 6,459,717. F atoms from an NF_3/He discharge are converted to Cl atoms by DCl. Cl + HI supplies ground-state iodine, and Cl + HN_3 → N_3 followed by Cl + N_3 produces NCl($a^1\Delta$), which pumps I($^2P_{1/2}$) in the gain region.

Practical points. Hydrazoic acid is toxic and explosive in concentrated form, which is why it is stored and handled diluted in helium. Because the carrier is all gas, AGIL avoids COIL's water vapor and liquid handling. The price is a more complex radical chemistry, in which unwanted Cl, N_3, and NCl(a) self-reactions compete with the pumping step.

Connection to the N + NI proposal. AGIL is the closest relative of the N + NI scheme considered in this paper. Both use nitrogen–halogen radical chemistry in a flow, and both depend on a metastable energy carrier that transfers its energy to atomic iodine. The difference is the target level. AGIL pumps the 0.94 eV I($^2P_{1/2}$) level and lases at 1.315 μm. The N + NI scheme aims at the 6.95 eV $5p^4(^3P_2)6s$ level and the 206.2 nm line, which needs about seven times more energy per iodine atom.

The 206.2 nm Iodine Line: Sources, Excitation Mechanisms, and a Proposed N + NI Experiment

The N + NI scheme proposed earlier depends on the iodine line at 206.2 nm, which runs from the $5p^4(^3P_2)6s\ ^2[2]_{3/2}$ level to I($5p^5\ ^2P°_{1/2}$). This line has a long history as a photochemical light source, and that history bears directly on how to excite it chemically.

The Harteck–Reeves–Thompson iodine lamp (1964)

Purpose. Harteck, Reeves, and Thompson at Rensselaer developed the iodine lamp to excite carbon monoxide selectively into its metastable $a^3\Pi$ state.[18] The 2062 Å iodine line falls just inside the (0,0) band of the CO Cameron system ($X^1\Sigma^+ \rightarrow a^3\Pi$, band at 2059.6 Å). At this wavelength CO absorbs weakly but usefully (absorption coefficient 0.0076 cm^{-1} at one atmosphere and room temperature). CO_2, O_2, N_2, and H_2O absorb less than 10^{-4} cm^{-1}, so excited CO could be studied without interference.

Why iodine works as a monochromatic source. The atomic iodine spectrum has no lines between 2062 Å and 3552 Å, and the next lines to shorter wavelength are at 1876, 1844, and 1830 Å. With a suitable window or filter, the lamp is therefore almost monochromatic at 2062 Å. Iodine's vapor pressure at room temperature, about 0.3 torr, is also convenient for a discharge. The authors identified the line as $6s\ ^2P_{3/2} \rightarrow 5p^5\ ^2P_{1/2}$, a non-resonance transition; this is the label used in the 1974 typescript.

Construction (Fig. 8). Two lamps were built.

- **Small lamp.** A discharge tube about 15 cm (6 in) long, with a quartz window at one end, run with either electrodes or an electrodeless discharge. It was used to measure absorption coefficients over a 94 cm path. Reagent-grade iodine was purified by fractional distillation in a side arm. The most persistent impurity, water vapor, made the discharge erratic and produced strong OH bands until it was removed.
- **Photochemical lamp.** Two concentric cylinders about 100 cm long:
  - **Inner tube:** quartz, carrying the discharge.
  - **Outer jacket:** Pyrex, filled with the gas to be irradiated.
  - **Argon flow:** argon flowed continuously through the inner tube, picking up iodine vapor from a reservoir. It stabilized the discharge and buffered the electrodes against attack by iodine. An earlier static version without argon was much less satisfactory.
  - **Windows:** quartz windows at each end allowed the spectrum and output to be monitored.

Performance. The output was almost entirely 2062 Å radiation; the 1876 Å line was about 1/30 as intense, and the continua near 3000 Å were weak. The 2062 Å output was measured by ammonia actinometry: 150 torr of NH_3 in the outer jacket was irradiated, and the N_2 produced was measured by mass spectrometry, using Wiig's quantum yields. It came to 2×10^{18} quanta per second, about 2 W of 206 nm light. With CO at 200–700 torr in the jacket, CO_2 formed linearly with time, with a quantum efficiency between a few tenths and unity:

$$CO(X^1\Sigma^+) + h\nu(206.2\ nm) \rightarrow CO(a^3\Pi, v = 0)$$

$$CO(a^3\Pi) + CO \rightarrow CO_2 + C$$

The absorption by CO fell to about half its room-temperature value when the hot line from the large lamp was used. The cause is Doppler and pressure broadening of the iodine line, together with changes in the CO rotational populations; so the line's width, and hence the lamp temperature, matters.

Later developments at RPI and elsewhere. Liuti, Dondes, and Harteck used the lamp to make carbon suboxide (C_3O_2) photochemically from CO, and they reported isotopic enrichment in the photochemistry of CO with the 2062 Å line.[19] Liuti and Mentall later built a "monochromatic" version at NASA Goddard.[20] It used a 2450 MHz microwave discharge (about 50 W) in iodine vapor at about 0.5 torr, in a 2.5 cm diameter tube with Suprasil windows. A 1 cm gas cell of flowing propene served as a filter, absorbing the 1876, 1844, and 1830 Å lines while transmitting 2062 Å.

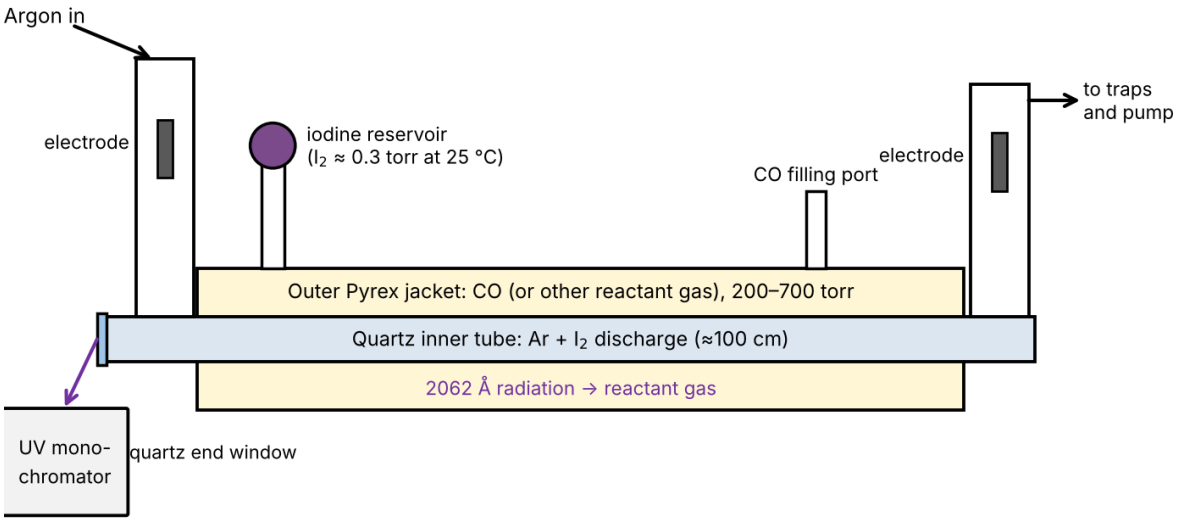


Figure 8. The Harteck–Reeves–Thompson photochemical iodine lamp (redrawn after Fig. 2 of ref. 18). Argon carries iodine vapor from the reservoir through the 100 cm quartz inner tube, where an electrode discharge excites the 2062 Å line. The reactant gas (CO) fills the surrounding Pyrex jacket, and a quartz end window lets a UV monochromator monitor the output.

Enhancement by rare-gas metastables: the Leiga–McInally flashlamp (1967)

Leiga and McInally (Xerox Research Laboratories) tried to pulse the iodine lamp and found that a flashlamp filled with pure iodine fired erratically.[21]

- **Lamps:** 9 mm Suprasil tubes with tungsten electrodes, holding iodine at its room-temperature vapor pressure (about 0.3 torr) and 5–240 torr of added rare gas.
- **Circuit:** a 150 μF capacitor discharged through a 150 μH inductor at 1–3 kV, giving pulses of about 0.6 ms.

Adding xenon or krypton increased the 206.2 nm emission enormously. The enhancement was about 400 with xenon (130 torr, 3 kV) and about 700 with krypton (120 torr, 3 kV), but only about 10 with argon.

Their explanation is a selective energy-transfer and cascade mechanism:

$$\mathrm{Xe}(1s_5,\ 8.315\ \mathrm{eV}) + \mathrm{I}(^2P_{3/2}) \rightarrow \mathrm{Xe} + \mathrm{I}(6p\ ^4P_{3/2}) \text{ (energy defect} \approx 6\ \mathrm{cm}^{-1}\text{, spin-allowed)}$$

$$\mathrm{Kr}(1s_5,\ 9.91\ \mathrm{eV}) + \mathrm{I}_2 \rightarrow \mathrm{Kr} + \mathrm{I}(^2P_{3/2}) + \mathrm{I}(6p\ ^4P_{3/2}) \text{ (requires 9.85 eV)}$$

$$\mathrm{I}(6p\ ^4P_{3/2}) \rightarrow \mathrm{I}(6s\ ^2[2]_{3/2}) + h\nu(911.4\ \mathrm{nm})$$

$$\mathrm{I}(6s\ ^2[2]_{3/2}) \rightarrow \mathrm{I}(5p^5\ ^2P^\circ_{1/2}) + h\nu(206.2\ \mathrm{nm})$$

Argon's metastables (11.55 eV) lie above the ionization energy of iodine, so they ionize it and give only a weak, unselective enhancement. For a 206.2 nm laser this mechanism matters: a near-resonant rare-gas metastable can feed the upper laser level selectively, through a cascade, without the electron-impact excitation that also populates the lower level.

$Xe–I_2$, $He–I_2$, and $Ar–I_2$ discharge excilamps (Tomsk, 2002)

The most thorough modern study of the 206.2 nm line as a lamp is by Lomaev and Tarasenko of the Institute of High Current Electronics in Tomsk.[22] They built sealed quartz lamps, with at least 70% transmission at 200 nm, excited in two ways (Fig. 9):

- **Glow discharge:** internal electrodes driven by a step-up transformer (AC or rectified).
- **Capacitive discharge:** external electrodes driven by high-voltage pulses at 10–100 kHz.

In some lamps a small box of solid iodine was attached to the discharge volume. As the coldest point of the lamp, its temperature set the iodine vapor pressure; it could be insulated or warmed by a small part of the discharge current to adjust it. This kept the iodine supply constant over the lamp's life.

Results.

- **Optimum pressure:** 0.1–20 torr for the glow discharge and no more than about 15 torr for the capacitive discharge at 20 kHz. At higher pressures the glow discharge contracted.
- **Buffer gas:** with equal buffer-gas and iodine pressures, the relative UV outputs were:

Lamp type	$Xe–I_2$	$He–I_2$	$He–Xe–I_2$	$Ne–I_2$	$Ar–I_2$
Glow discharge	1	0.9	0.85	—	0.1
Capacitive discharge (20 kHz)	0.9	1	0.7	0.4	0.1

- **Efficiency:** with $Xe–I_2$ and $He–I_2$, the UV efficiency reached about 12% for the glow lamps and about 9% for the capacitive lamps. With $Ar–I_2$ or iodine alone it was only a few percent or less.
- **Spectrum:** at low xenon pressure the 206.2 nm line dominated. Above about 10 torr, the XeI* B→X excimer band at 253 nm grew in.
- **Lifetime:** more than 1000 hours sealed.

The poor performance of argon matches Leiga and McInally's finding, and the good performance of xenon is consistent with their metastable-transfer mechanism. The mechanism for helium, whose metastables lie far above the iodine ionization energy, was not established.

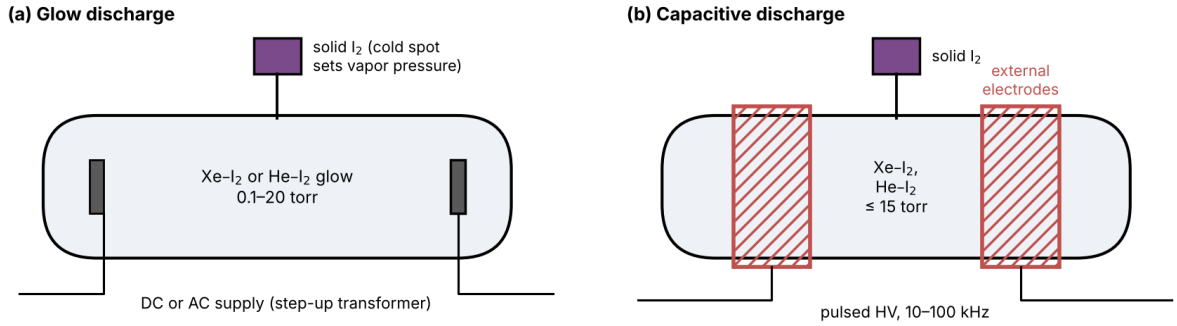


Figure 9. Iodine–rare-gas excilamps of Lomaev and Tarasenko (schematic, after ref. 22): (a) glow-discharge lamp with internal electrodes; (b) capacitive-discharge lamp with external electrodes. In both, a reservoir of solid iodine at the coldest point of the lamp sets the iodine vapor pressure.

A proposed apparatus for studying N + NI

The lamp studies show that the 206.2 nm upper level can be populated efficiently. The question for a chemical laser is whether the N + NI reaction populates it selectively, without filling the I($^2P_{1/2}$) lower level as fast. Figure 10 shows an apparatus designed to answer that question in a nitrogen-afterglow configuration, in which the discharge region and the reaction region are kept separate.

Nitrogen atoms. Purified N_2 (passed through a liquid-nitrogen trap) flows at a controlled rate through a water-cooled DC arc discharge in the upstream end of the flow system. The arc dissociates part of the N_2. The gas then passes through a light trap (a blackened bend) so that discharge light and ions do not reach the observation region. Downstream the flow carries ground-state N(^4S) atoms and the Lewis–Rayleigh afterglow, with no electric field present:

$$N_2 + e^- \rightarrow 2\ N + e^- \text{ (in the arc)}$$

$$N + N + M \rightarrow N_2(B^3\Pi_g) + M \rightarrow N_2(A^3\Sigma_u^+) + h\nu \text{ (first positive) (afterglow)}$$

The flow tube walls are coated with phosphoric acid (or the tube is Teflon-lined) to slow wall recombination of N atoms. The N-atom concentration is measured by the standard NO titration at an inlet just downstream of the light trap:

$$N + NO \rightarrow N_2 + O \text{ (fast; the afterglow is extinguished at the end point [NO] = [N])}$$

$$O + NO + M \rightarrow NO_2^* + M \rightarrow NO_2 + h\nu \text{ (yellow-green air afterglow beyond the end point)}$$

Iodine. Iodine vapor is supplied from a solid-iodine ampoule in a thermostatted bath, joined to the flow tube just downstream of the N-atom entrance but outside the discharge path. The iodine therefore never passes through the arc. This follows the lesson of the earlier lamps: Harteck, Reeves, and Thompson used argon to protect their electrodes from iodine, and Lomaev and Tarasenko set the iodine pressure with a cold-spot reservoir. The bath temperature sets the iodine pressure: roughly 0.03 torr at 0 °C, 0.3 torr at 25 °C, and about 1 torr at 40 °C. A needle valve, with an optional argon carrier, controls the iodine flow. Moving the iodine and NO injection points along the tube changes the reaction time, $t = z/v$.

Reactions to be studied.

$$N + I_2 \rightarrow NI + I$$

$$N + NI \rightarrow N_2 + I(5p^4 6s\ ^2[2]_{3/2}) \text{ (proposed pumping step; ≈ 190 kcal/mol available)}$$

$$N + NI \rightarrow N_2(A, B) + I \text{ (competing channel; energy transfer to } I_2 \text{ gives the blue fluorescence)}$$

$$I(6s\ ^2[2]_{3/2}) \rightarrow I(5p^5\ ^2P^\circ_{1/2}) + h\nu(206.2\text{ nm})$$

$$I(^2P_{1/2}) + O_2 \rightleftharpoons I(^2P_{3/2}) + O_2(a^1\Delta_g) \text{ (optional lower-level quenching)}$$

$$I + I + M \rightarrow I_2 + M$$

Diagnostics (Fig. 10). The observation zone, just downstream of the iodine inlet, has MgF_2 or Suprasil windows on three sides:

1. **VUV monochromator and photomultiplier,** evacuated or N_2-purged, recording the 206.2 nm emission and the shorter iodine lines at 183.0 and 178.3 nm as functions of [N], [I_2], pressure, and reaction time.
2. **206.2 nm absorption probe:** a Harteck–Reeves–Thompson iodine lamp shines across the zone. Absorption of its 206.2 nm line measures the concentration of the lower level, I($^2P_{1/2}$),

directly. If the upper level ever becomes more populated per state than the lower level, the measured absorption turns into gain.

3. **Visible and near-infrared spectrometer with a germanium detector:** records the N_2 first-positive afterglow, the I_2 blue fluorescence, and the 1.315 μm emission of $I(^2P_{1/2})$. The 1.315 μm signal is a second, independent measure of the lower-level population.

An optional O_2 inlet downstream of the iodine allows a test of the resonance-quenching idea: the 1.315 μm emission should fall while the 206.2 nm emission is unaffected. Downstream, a liquid-nitrogen trap removes iodine and other condensable products before the throttle valve, pressure gauge, and pump.

What the experiment would establish.

- **Branching fraction:** the fraction of N + NI reactive events that produce $I(6s\ ^2[2]_{3/2})$, from the 206.2 nm photon yield measured against NO-titrated [N].
- **Lower-level population:** the rate at which $I(^2P_{1/2})$ builds up, from the 206.2 nm absorption and the 1.315 μm emission.
- **Quenching:** whether added O_2 can hold $I(^2P_{1/2})$ low enough to satisfy $N_u > 2N_l$.

These three numbers show how close N + NI comes to the requirements derived in the following subsections. As shown there, the prospects for an actual inversion are poor.

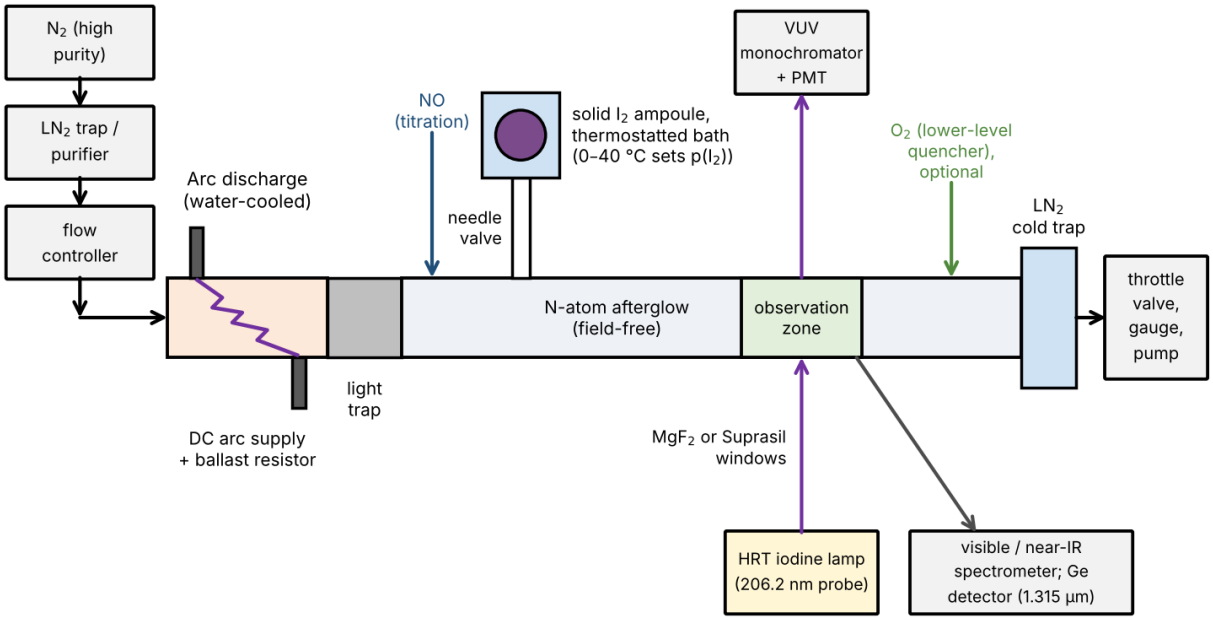


Figure 10. Proposed nitrogen-afterglow apparatus for studying the N + NI reaction. N atoms made in a water-cooled DC arc pass through a light trap into a field-free, H_3PO_4-coated flow tube. Iodine vapor from a thermostatted solid-iodine ampoule enters just downstream of the N-atom entrance, outside the discharge path. NO titration measures [N]. The observation zone is viewed by a VUV monochromator, probed at 206.2 nm by an iodine lamp, and monitored in the visible and near-IR (1.315 μm). An optional O_2 inlet tests lower-level quenching.

Flow-tube kinetics and the choice of observation position

The NI needed for the pumping step is not supplied directly; it is made in the flow tube by N + I_2. What is observed at any point downstream of the iodine inlet is therefore the outcome of two consecutive reactions:

$$N + I_2 \rightarrow NI + I \ (k_1)$$

$$N + NI \rightarrow N_2 + I(6s\ ^2[2]_{3/2}) \text{ or } N_2(A, B) + I \ (k_2)$$

together with the slower losses of N atoms by recombination and at the wall:

$$N + N + M \rightarrow N_2 + M \ (k_{NN} \approx 1 \times 10^{-32}\ cm^6\ s^{-1})$$

$$N \rightarrow \text{wall} \ (k_w \approx 5\ s^{-1} \text{ on an } H_3PO_4\text{-coated wall})$$

$$I + I + M \rightarrow I_2 + M$$

No measured rate constants were found for N + I_2 or N + NI. In the analysis below, k_1 is therefore treated as an unknown between 10^{-13} and 10^{-11} $cm^3\ s^{-1}$. k_2 is taken as 10^{-10} $cm^3\ s^{-1}$, typical of radical–radical reactions.

Pseudo-first-order solution. In plug flow at velocity v, distance z corresponds to reaction time $t = z/v$. If N is kept in excess over I_2, [N] is nearly constant through the reaction zone, and the two steps are pseudo-first-order with rates $k_1' = k_1[N]$ and $k_2' = k_2[N]$. The standard consecutive-reaction solution gives

$$[NI](t) = [I_2]_0 \frac{k_1'}{k_2' - k_1'}\left(e^{-k_1' t} - e^{-k_2' t}\right)$$

and the rate of the N + NI step, which is proportional to the 206.2 nm emission, is

$$R_2(t) = k_2[N][NI] \approx k_1[N][I_2]_0\, e^{-k_1[N]t} \qquad (k_2 \gg k_1,\ t \gg 1/k_2[N])$$

NI is thus a short-lived intermediate in quasi-steady state, $[NI] \approx (k_1/k_2)[I_2]$. The N + NI rate simply follows the rate at which N + I_2 uses up the iodine, and each I_2 molecule gives one N + NI event. Three distances describe the profile:

$$z_2 = \frac{v}{k_2[N]}, \qquad z^* = \frac{v \ln(k_2/k_1)}{(k_2 - k_1)[N]}, \qquad z_1 = \frac{v}{k_1[N]}$$

These are the rise length, the position of the emission maximum, and the decay length. With [N] = 10^{14} cm^{-3} and v = 10 m/s, $z_2 \approx 1$ mm and z^* is less than 1 cm for any k_1 in the range considered. The decay length is 1, 10, or 100 cm for $k_1 = 10^{-11}$, 10^{-12}, or 10^{-13} $cm^3\ s^{-1}$. Only this decay can be resolved spatially in practice.

Mixing. The iodine does not mix with the N-atom stream instantly. The slowest radial diffusion mode in a tube of radius r decays with time constant

$$\tau_{mix} \approx \frac{r^2}{5.78\, D}, \qquad z_{mix} = v\, \tau_{mix}$$

For I_2 in N_2 at 2 torr, D ≈ 28 $cm^2\ s^{-1}$ (scaled from about 0.075 $cm^2\ s^{-1}$ at one atmosphere). In a 2.5 cm diameter tube at 10 m/s this gives $z_{mix} \approx 10$ cm for injection at the axis and roughly 2–3 cm for a

ring or multi-hole injector, which halves the radial distance. Upstream of z_{mix}, the reaction and the mixing overlap, and the measured profile cannot be interpreted with plug-flow kinetics.

Numerical model (Fig. 11). The full set of reactions above was integrated along the flow for 2 torr N_2 at 300 K and 10 m/s.

- **Panel (a):** the base case. NI rises within about a millimeter to a quasi-steady level about 100 times below $[I_2]$. I_2 is used up over the decay length, and the freed iodine atoms recombine only slowly.
- **Panel (b):** the effect of k_1. If $k_1 \approx 10^{-11}$ cm^3 s^{-1}, almost all the iodine reacts inside the mixing zone.
- **Panel (c):** if $[I_2]_0$ approaches $[N]_0$, the iodine (which consumes two N atoms per I_2) uses up the nitrogen atoms and cuts the emission short.
- **Panel (d):** a design map. It shows the peak position and the decay length as functions of $[N]_0$ against the mixing-length band.

Iodine-atom recycling through N + I + M → NI + M had no visible effect at these iodine concentrations, even with a rate constant as large as 10^{-32} cm^6 s^{-1}.

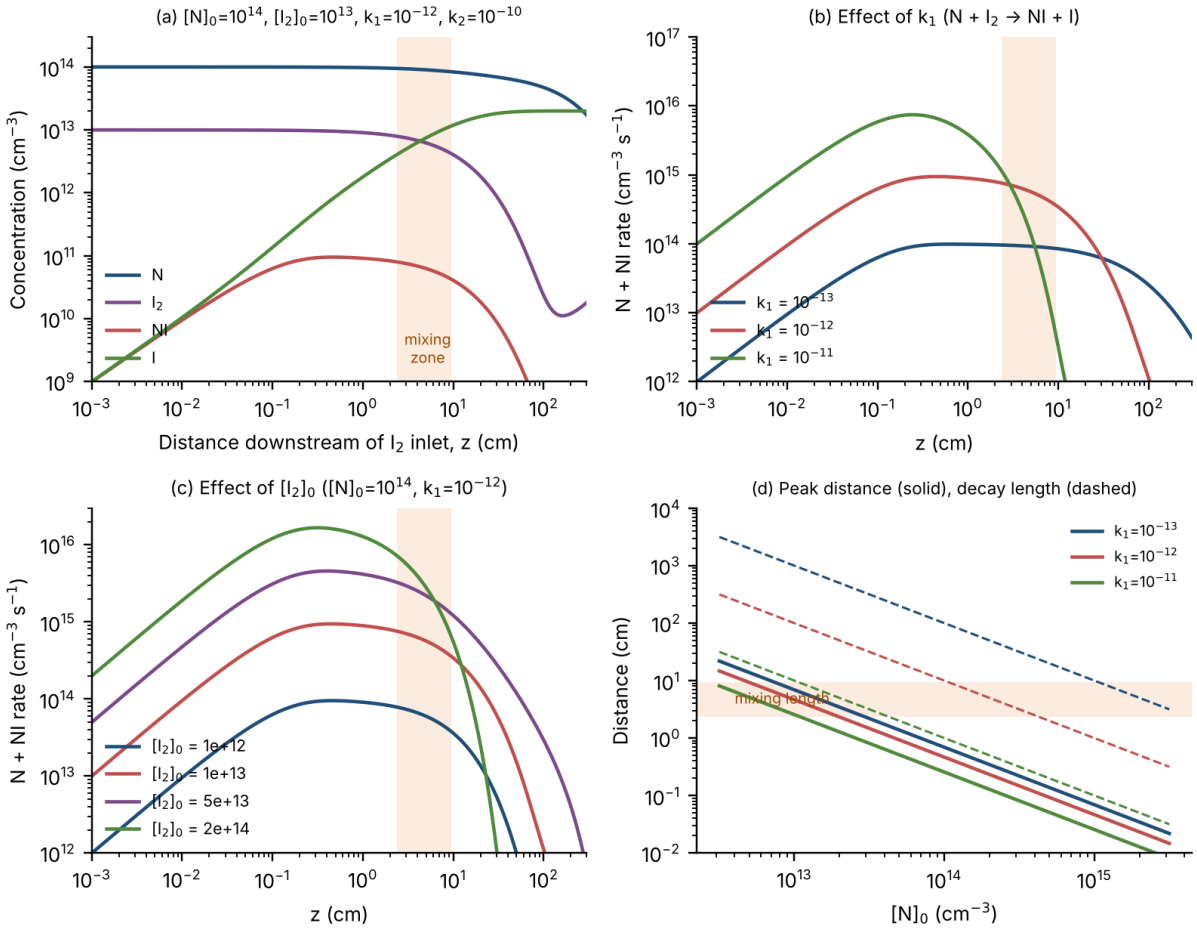


Figure 11. Modeled kinetics of N + I_2 → NI + I followed by N + NI in the proposed flow tube (2 torr N_2, 300 K, plug flow at 10 m/s; $k_2 = 10^{-10}$ cm^3 s^{-1}; N recombination and wall loss included). (a) Concentrations for $[N]_0 = 10^{14}$ cm^{-3}, $[I_2]_0 = 10^{13}$ cm^{-3}, $k_1 = 10^{-12}$ cm^3 s^{-1}. (b) N + NI reaction rate for three values of k_1. (c) Effect of the initial I_2 concentration. (d)

Distance to the emission maximum (solid) and decay length $v/(k_1[N])$ (dashed) as functions of $[N]_0$. The shaded band is the estimated I_2 mixing length (2–10 cm).

Design rules for the experiment.

1. **Observe just beyond the mixing length,** about 3–10 cm downstream of the iodine inlet in the configuration above, and choose conditions so that the decay length z_1 is two to three times z_{mix}.
2. **If N + I_2 proves fast** ($k_1 \approx 10^{-11}$ cm^3 s^{-1}), most of the reaction takes place before the iodine is mixed. Lower [N] to about 10^{13} cm^{-3}, increase the flow velocity, or reduce the pressure, which increases D and shortens z_{mix}.
3. **Keep N in five- to ten-fold excess,** that is $[I_2] \approx 10^{12}$–10^{13} cm^{-3} for $[N] \approx 10^{14}$ cm^{-3}. This is far below the iodine vapor pressure even at 0 °C (about 10^{15} cm^{-3}), so the needle valve and the dilution into the main flow, not the bath temperature alone, set $[I_2]$. The iodine flow should be calibrated, for example by visible absorption of I_2 near 500 nm.
4. **Fixed window, movable injector.** Keep the observation window fixed and move the iodine injector, so that the optics and detection efficiency do not change from point to point.

What the profile measures. Because NI follows the iodine, the 206.2 nm emission decays as

$$I_{206}(z) \propto \phi\, k_1[\mathrm{N}][\mathrm{I_2}]_0 \exp\left(-\frac{k_1[\mathrm{N}]\, z}{v}\right)$$

where φ is the fraction of N + NI events that produce I(6s $^2[2]_{3/2}$). With [N] from the NO titration, the slope of ln I_{206} against z gives k_1 directly. The absolute 206.2 nm photon yield then gives φ, the quantity that decides whether a 206.2 nm laser based on N + NI is feasible. The analysis assumes $k_2 \gg k_1$. If N + NI were slow instead, NI would build up, the emission maximum would move downstream, and the profile would show a clear rise before the decay; that rise would itself measure k_2.

Would adding Xe or Kr to the N_2 arc enhance the 206.2 nm emission?

The lamp studies above show that metastable xenon and krypton raise the 206.2 nm intensity by factors of several hundred. It is therefore natural to ask whether adding Xe or Kr to the N_2 in the arc would carry extra excitation downstream to the reaction zone. The analysis below indicates that it would not. The obstacle is not the radiative lifetime of the excited rare-gas atoms but their collisional destruction in transit, together with their reaction with I_2.

Radiative lifetime is not the limit. The relevant states, Xe($^3P_2$) at 8.315 eV and Kr($^3P_2$) at 9.91 eV, are metastable. In isolation they survive for seconds, which is why they transfer energy so effectively inside the Leiga–McInally flashlamp. The short-lived resonance levels ($^3P_1$) radiate quickly, but in a discharge their radiation is trapped and their population ends up largely in the metastable levels.

Losses between the arc and the iodine inlet.

1. **Wall deactivation.** A metastable rare-gas atom is deactivated at essentially every wall collision. For Xe* in N_2 at 2 torr, the diffusion coefficient is estimated at about 40–50 cm^2 s^{-1} (scaled from about 0.12 cm^2 s^{-1} at one atmosphere). The time to diffuse to the wall of a 2.5 cm diameter tube is then $\tau_{wall} \approx r^2/(5.78\ D) \approx 6$–$7$ ms. The 15–20 cm transit from the arc to

the iodine inlet takes about 20 ms at 10 m/s, so even without any gas-phase loss only a few percent would survive:

$$\frac{[\mathrm{Xe}^*](z)}{[\mathrm{Xe}^*]_0} \approx \exp\left(-\frac{z}{v\,\tau_{wall}}\right) \approx e^{-3}$$

The light-trap bend, which forces contact with the wall, would remove most of the remainder.

2. **Gas-phase quenching.** Along the way the metastables collide with about 6×10^{16} cm^{-3} of N_2 and about 10^{14} cm^{-3} of N atoms:

$$\mathrm{Xe}(^3P_2) + N_2 \rightarrow \mathrm{Xe} + N_2(B^3\Pi_g) \text{ (exothermic by about 1 eV)}$$

$$\mathrm{Kr}(^3P_2) + N_2 \rightarrow \mathrm{Kr} + N_2^*$$

$$\mathrm{Xe}(^3P_2), \mathrm{Kr}(^3P_2) + \mathrm{N} \rightarrow \text{quenching}$$

Velazco, Kolts, and Setser measured the 300 K quenching rate constants of Ar, Kr, and Xe metastables by many small molecules.[25] Even a slow quenching constant of 10^{-13} cm^3 s^{-1} by N_2 would give a lifetime under 200 μs, or about 2 mm of flow at 10 m/s.

3. **No re-excitation in the afterglow.** In the flashlamp, the discharge continuously regenerated metastables where the iodine was. The afterglow cannot do this: its main energy carrier, $N_2(A^3\Sigma_u^+)$ at 6.2 eV, lies below the lowest Xe excited level (8.3 eV).

Reaction with I_2 at the inlet. Any metastables that did reach the iodine inlet would meet I_2 before iodine atoms. Leiga and McInally pointed out that $\mathrm{Xe}(^3P_2) + I_2$ can give one ground-state iodine atom and one in a 6s level lying below the 206.2 nm upper level. That channel uses up the xenon energy without enhancing the 2062 Å line.[21] The XeI* excimer band at 253 nm, which dominates the Xe–I_2 lamps at higher pressure,[22] shows that excimer formation is another important channel:

$$\mathrm{Xe}(^3P_2) + I_2 \rightarrow \mathrm{Xe} + \mathrm{I}(^2P_{3/2}) + \mathrm{I}(6s, \text{ below the 206.2 nm upper level})$$

$$\mathrm{Xe}(^3P_2) + I_2 \rightarrow \mathrm{XeI}(B) + \mathrm{I} \text{ (XeI B→X emission at 253 nm)}$$

$$\mathrm{Kr}(^3P_2) + I_2 \rightarrow \mathrm{Kr} + \mathrm{I}(^2P_{3/2}) + \mathrm{I}(6p\ ^4P_{3/2}) \text{ (requires 9.85 eV)}$$

The krypton channel does feed the 206.2 nm upper level through the 6p → 6s cascade. However, it works only where Kr* is produced continuously, as inside a discharge. The Xe–I_2 and He–I_2 excilamps of Lomaev and Tarasenko[22] also operate with the excitation inside the discharge itself.

Effect on the N-atom source. Xenon would also degrade the arc. Its ionization energy (12.1 eV) is lower than that of N_2 (15.6 eV), and its excited levels begin at 8.3 eV, so it would take electron energy that would otherwise dissociate N_2 and would lower the electron temperature. The result would be fewer N atoms and no useful metastables downstream.

The cascade fills the lower level too. Even where rare-gas transfer works, it populates 6p $^4P_{3/2}$, which cascades through the 911.4 nm line into the 206.2 nm upper level. Every 206.2 nm photon then deposits an atom in $\mathrm{I}(^2P_{1/2})$, the lower laser level. That is ideal for a lamp, but it does not by itself produce the inversion $N_u > 2N_l$ needed for gain, so the lower-level problem identified earlier remains.

Recommended tests.

- **Diagnostic check.** In the apparatus of Fig. 10, add a few percent of Xe to the N_2 and look at the observation zone for Xe lines or the 253 nm XeI band. Their absence would confirm that

no metastables reach the reaction zone, and the run would also show how much Xe reduces the N-atom yield measured by NO titration.

- **Separate comparison experiment.** To compare rare-gas pumping with N + NI pumping directly, generate the metastables where the iodine is: for example a weak capacitive or pulsed discharge in Xe/I_2 or Kr/I_2 in the observation zone, probed with the same 206.2 nm absorption lamp. This would measure the upper- and lower-level populations produced by the cascade route, for direct comparison with those from N + NI.

The lower-level removal requirement and the prospects for inversion

The earlier discussion suggested that a near-resonant quencher such as O_2 might empty the $I(^2P_{1/2})$ lower level fast enough to sustain gain at 206.2 nm. That suggestion can now be made quantitative, and the result is discouraging.

Steady-state condition. Let the upper level, $I(6s\ ^2[2]_{3/2})$, be pumped at rate P and decay radiatively with lifetime τ_u. A fraction b of its decays go to $I(^2P_{1/2})$ at 206.2 nm, and the rest go to the ground state at 178.3 nm. The lower level is removed by a quencher Q at rate $k_q[Q]$. In steady state

$$N_u = P\,\tau_u, \qquad N_l = \frac{b\,P}{k_q[\mathrm{Q}]}$$

and gain requires $N_u > 2N_l$ (degeneracies 4 and 2), that is

$$k_q[\mathrm{Q}] > \frac{2b}{\tau_u}$$

The pump rate cancels. However strongly N + NI pumps the upper level, the lower level must be emptied at a rate comparable to the radiative decay rate of the upper level itself.

Numbers. The transition probabilities of the 206.2 and 178.3 nm lines were not available for this revision, so τ_u is bracketed at 3–30 ns, typical for allowed transitions at these wavelengths. b is bracketed at 0.3–1; the upper end applies because ground-state iodine traps the 178.3 nm resonance radiation and pushes more decays into the 206.2 nm channel. For O_2, the rate constant is that of the reverse of the COIL pumping step, $k_r = k_f/K_{eq} \approx 7.8 \times 10^{-11}/2.86 \approx 2.7 \times 10^{-11}$ cm^3 s^{-1} at 300 K.[17]

τ_u (ns)	b	Removal rate $2b/\tau_u$ (s^{-1})	O_2 needed (torr)	Gas-kinetic quencher needed (torr)
3	0.3	2×10^8	≈ 230	≈ 21
3	1.0	7×10^8	≈ 760	≈ 69
10	0.3	6×10^7	≈ 68	≈ 6
10	1.0	2×10^8	≈ 230	≈ 21
30	0.3	2×10^7	≈ 23	≈ 2
30	1.0	7×10^7	≈ 76	≈ 7

Table 2. Lower-level removal rate needed for gain on the 206.2 nm line, and the corresponding quencher pressure at 300 K for O_2 ($k_r = 2.7 \times 10^{-11}$ cm^3 s^{-1}) and for a hypothetical gas-kinetic quencher (3×10^{-10} cm^3 s^{-1}).

Three consequences follow.

1. **Pressure.** Tens to hundreds of torr of O_2 are needed, against an afterglow operating pressure of about 2 torr. Even the fastest conceivable quencher needs several torr or more.
2. **Selectivity.** At such densities O_2, an efficient quencher of high-lying electronic states, would be expected to quench the 6.95 eV upper level as well. The near-resonance that favors removal of the lower level offers no protection to the upper level.
3. **Gain magnitude.** Even with perfect lower-level removal, the upper-level population is only $N_u = P\,\tau_u$. The flow-tube model gives $P \approx 10^{15}$–10^{16} cm^{-3} s^{-1} even if every N + NI event reached the upper level, so $N_u \approx 10^6$–10^8 cm^{-3}. With an effective stimulated-emission cross section of about 10^{-13} cm^2 (the Doppler-limited value of about 3×10^{-13} cm^2 for $A \approx 3 \times 10^7$ s^{-1}, reduced for the ^{127}I hyperfine structure), the gain is at most about 3×10^{-5} cm^{-1}. A 1 m resonator with 1% round-trip loss needs about 5×10^{-5} cm^{-1}. Reaching threshold would require $P \gtrsim 10^{17}$–10^{18} cm^{-3} s^{-1}, 10–1000 times what the afterglow can supply.

Pulsed operation. Pulsed operation does not avoid the problem. Without removal, the lower-level population catches up with the upper level within about $\tau_u/(2b)$, a few nanoseconds after pumping begins. Self-terminating lasers such as the N_2 laser at 337 nm succeed only because electron impact pumps them on nanosecond timescales. A chemical pump acting over microseconds to milliseconds cannot.

The calculations behind Table 2 and the gain estimate are collected in the spreadsheet "O2 Lower-Level Removal Requirement.xlsx," in which the lifetime, branching fraction, rate constants, and cavity parameters can be varied.

Conclusion

Chemical lasers are related to kinetics in two ways. First, knowledge of a system's kinetics allows one to predict whether a chemical laser is possible; here kinetics is the tool of the person building the laser. Second, kinetic data, particularly on energy transfer and on energy distributions in reaction products, can be obtained by analyzing laser emission as a function of various parameters. Unambiguous results are hard to obtain, however, because the systems are often very complex. Also, the number of systems that can be studied this way is, to date, fairly small.

Conclusions to date on a 206.2 nm N + NI laser. The analysis added in this revision sharpens the 1974 proposal and shows that the central difficulty is obtaining an inversion, not finding a pump.

1. **The pump is energetically adequate.** N + NI releases about 190 kcal/mol, more than the 6.95 eV needed to reach I($5p^4(^3P_2)6s\ ^2[2]_{3/2}$). The lamp literature (Harteck–Reeves–Thompson, Leiga–McInally, Lomaev–Tarasenko) shows that this level can be populated efficiently and emits strongly at 206.2 nm.
2. **The lower level is the obstacle.** Every 206.2 nm photon deposits an atom in I($5p^5\ ^2P^\circ_{1/2}$). This level is metastable (radiative lifetime about 0.1 s), whereas the upper level radiates in nanoseconds. Gain requires the lower level to be emptied at a rate of order $2b/\tau_u \approx 10^7$–10^9 s^{-1}, independent of the pump rate.
3. **Collisional removal is not adequate.** O_2, the most selective known quencher of I($^2P_{1/2}$), would be needed at tens to hundreds of torr. At that density it would very likely quench the upper level too, and it is incompatible with a 2 torr nitrogen afterglow. No gas-kinetic quencher brings the requirement down to the afterglow pressure range.

4. **The pump rate is too low even with perfect removal.** N + NI in an afterglow can supply at most about 10^{15}–10^{16} upper-level atoms cm^{-3} s^{-1}, giving gain below 10^{-4} cm^{-1}. Threshold in a practical resonator needs 10–1000 times more.
5. **Pulsed operation does not help.** Without removal, the lower level catches up within nanoseconds, far faster than a chemical pump can act.
6. **Rare-gas additives do not help in the afterglow.** Xe and Kr metastables enhance 206.2 nm emission only where a discharge regenerates them. In the afterglow they would be destroyed at the walls and in collisions before reaching the iodine, and the cascade they drive fills the lower level as well.

The proposed experiment therefore remains worthwhile, but as a measurement rather than a laser test. Its value lies in the N + I_2 rate constant, the fraction of N + NI events that populate the 206.2 nm upper level, and the rate at which the lower level builds up. These quantities would characterize an unusual, highly exothermic atom–radical reaction and test the energy-disposal ideas behind it. An inversion at 206.2 nm would need a fundamentally different approach: excitation on a nanosecond timescale, as in self-terminating discharge lasers, or a lower-level removal process orders of magnitude faster than any known collisional quencher.

In the 1974 paper's own terms, kinetics here serves in both roles at once: it predicts that a 206.2 nm laser based on N + NI is very unlikely, and it identifies exactly which measured quantities would confirm or overturn that prediction.

Postscript: Developments Since 1974

Several points in this paper were overtaken by later work.

- **Continuous-wave HF and DF lasers.** The supersonic-mixing CW HF laser (Fig. 5) first operated in 1969,[10] and combustion-driven HF/DF lasers were later scaled to very high powers. The Mid-Infrared Advanced Chemical Laser (MIRACL), a megawatt-class DF device, first lased in 1980.[12]
- **Electronic-transition chemical lasers.** The statement that no chemical laser operated on an electronic transition was true in 1974, but not for long. In 1978 McDermott and co-workers demonstrated the chemical oxygen–iodine laser (COIL). In COIL, $O_2(a^1\Delta_g)$, produced by reacting Cl_2 with basic hydrogen peroxide, transfers its energy to atomic iodine, which lases at 1.315 μm.[11] This is the near-resonant exchange discussed above, used as a pump rather than as a quencher (see the COIL section and Fig. 6).
- **Megawatt-class COIL.** A megawatt-class COIL built from six modules was the weapon of the U.S. Airborne Laser (YAL-1).[13] It destroyed a ballistic missile in a test in February 2010, and the program was cancelled in December 2011.
- **All-gas-phase iodine laser (AGIL).** $NCl(a^1\Delta)$, an isovalent analog of $O_2(a^1\Delta_g)$ made from Cl + HN_3 chemistry, was later used to pump atomic iodine in an all-gas-phase iodine laser[14] (see the AGIL section and Fig. 7). Like the N + NI scheme proposed here, AGIL uses nitrogen–halogen chemistry to excite iodine, although it lases on the 1.315 μm transition rather than at 206.2 nm.

References

1. J. C. Polanyi, *J. Chem. Phys.* **34**, 347 (1961).
2. J. V. V. Kasper and G. C. Pimentel, *Phys. Rev. Lett.* **14**, 352 (1965).
3. C. H. Bamford and C. F. H. Tipper, eds., *Comprehensive Chemical Kinetics*, Vol. 3: *The Formation and Decay of Excited Species* (Elsevier, Amsterdam, 1969), p. 171.
4. K. G. Anlauf et al., *Discuss. Faraday Soc.* **44**, 183 (1967).
5. L. E. Brus and M. C. Lin, *J. Phys. Chem.* **75**, 2546 (1971).
6. T. D. Padrick and G. C. Pimentel, *J. Chem. Phys.* **51**, 91 (1969).
7. C. G. Freeman and L. F. Phillips, *J. Phys. Chem.* **68**, 362 (1964).
8. L. F. Phillips, *Can. J. Chem.* **43**, 369 (1965).

References added in the 2026 revision:

9. J. C. Polanyi, "Vibrational–rotational population inversion," *Appl. Opt. Suppl.* **2** (Chemical Lasers), 109 (1965).
10. D. J. Spencer, T. A. Jacobs, H. Mirels, and R. W. F. Gross, *Int. J. Chem. Kinet.* **1**, 493 (1969).
11. W. E. McDermott, N. R. Pchelkin, D. J. Benard, and R. R. Bousek, *Appl. Phys. Lett.* **32**, 469 (1978).
12. DARPA, "MIRACL," Innovation Timeline, https://www.darpa.mil/about/innovation-timeline/miracl.
13. "The Airborne Laser shoots for ballistic missile defense," *Laser Focus World* (January 2004).
14. U.S. Patent 6,459,717, "Continuous wave all gas phase iodine laser (AGIL)," T. L. Henshaw, G. D. Hager, M. R. Berman, and T. J. Madden, assigned to the U.S. Air Force (filed 2000, issued 2002).
15. N. Cohen and J. F. Bott, "A Review of Rate Coefficients in the H_2–F_2 Chemical Laser System," Aerospace Corp. Report SAMSO-TR-76-82 (1976); DTIC ADA024332.
16. G. Hancock, B. A. Ridley, and I. W. M. Smith, *J. Chem. Soc., Faraday Trans. 2* **68**, 2117 (1972). Reaction enthalpy from the theoretical study of O + CS → CO + S archived at hdl.handle.net/2445/163617 (Universitat de Barcelona).
17. V. N. Azyazov, "Excited states in the active media of oxygen–iodine lasers," *Quantum Electron.* **39**, 989 (2009).
18. P. Harteck, R. R. Reeves, Jr., and B. A. Thompson, "The Iodine Lamp: A Light Source for Selective Excitation of CO," *Z. Naturforsch.* **19a**, 2 (1964).
19. G. Liuti, S. Dondes, and P. Harteck, "Photochemical Production of C_3O_2 from CO," *J. Chem. Phys.* **44**, 4051 (1966); "Isotopic Enrichment in the Photochemistry of CO with the 2062-Å Iodine Line," *J. Chem. Phys.* **44**, 4052 (1966).
20. G. Liuti and J. E. Mentall, "Monochromatic Iodine Lamp," *Rev. Sci. Instrum.* **39**, 1767 (1968).
21. A. G. Leiga and J. A. McInally, "Enhancement of the 2062-Å Atomic-Iodine Line in an Iodine Inert-Gas Flashlamp," *J. Opt. Soc. Am.* **57**, 317 (1967).
22. M. I. Lomaev and V. F. Tarasenko, "Xe(He)–I_2 glow and capacitive discharge excilamps," *Proc. SPIE* **4747**, 390 (2002).

23. G. C. Manke, C. B. Cooper, S. C. Dass, T. J. Madden, and G. D. Hager, "A multiwatt all gas-phase iodine laser (AGIL)," *IEEE J. Quantum Electron.* (2003), doi:10.1109/JQE.2003.814381.

24. U.S. Patent 7,453,917, "Supersonic all gas-phase iodine laser," C. B. Cooper, G. C. Manke, G. D. Hager, and T. J. Madden (2008).

25. J. E. Velazco, J. H. Kolts, and D. W. Setser, "Rate constants and quenching mechanisms for the metastable states of argon, krypton, and xenon," *J. Chem. Phys.* **69**, 4357 (1978).